Separation Science and Technology
Publication details, including instructions for authors and subscription information:
http://www.informaworld.com/smpp/title~content=t713708471

Heater Effects on Cyclone Performance for the Separation of Solids from High Temperature and Pressure Effluents

Chrysi S. Laspidou[a]; Desmond F. Lawler[b]; Earnest F. Gloyna[b]; Bruce E. Rittmann[a]
[a] NORTHWESTERN UNIVERSITY, EVANSTON, ILLINOIS, USA [b] DEPARTMENT OF CIVIL ENGINEERING, UNIVERSITY OF TEXAS AT AUSTIN, AUSTIN, TEXAS, USA

Online publication date: 20 October 1999

To cite this Article Laspidou, Chrysi S. , Lawler, Desmond F. , Gloyna, Earnest F. and Rittmann, Bruce E.(1999) 'Heater Effects on Cyclone Performance for the Separation of Solids from High Temperature and Pressure Effluents', Separation Science and Technology, 34: 15, 3059 — 3076
To link to this Article: DOI: 10.1081/SS-100100822
URL: http://dx.doi.org/10.1081/SS-100100822

SEPARATION SCIENCE AND TECHNOLOGY, **34**(15), pp. 3059–3076, 1999

Heater Effects on Cyclone Performance for the Separation of Solids from High Temperature and Pressure Effluents

CHRYSI S. LASPIDOU*
ENVIRONMENTAL ENGINEERING PROGRAM
NORTHWESTERN UNIVERSITY
2145 SHERIDAN ROAD, EVANSTON, ILLINOIS 60208-3109, USA

DESMOND F. LAWLER and EARNEST F. GLOYNA
ENVIRONMENTAL HEALTH ENGINEERING PROGRAM
DEPARTMENT OF CIVIL ENGINEERING
UNIVERSITY OF TEXAS AT AUSTIN
AUSTIN, TEXAS 78712, USA

BRUCE E. RITTMANN
ENVIRONMENTAL ENGINEERING PROGRAM
NORTHWESTERN UNIVERSITY
2145 SHERIDAN ROAD, EVANSTON, ILLINOIS 60208-3109, USA

ABSTRACT

A 25.4-mm diameter hydrocyclone with an underflow receiver was evaluated for its ability to achieve separation of fine particles from water at elevated temperatures and pressures relevant to supercritical oxidation. Temperature was varied from 25°C to 340°C, while pressure was maintained at 27.6 MPa. The particles studied were α-alumina. Particle-removal efficiency was affected by the separation capabilities of the hydrocyclone, deposition on the heater surface, and flocculation of the particles. Particle-size distributions and suspended solids analyses confirmed that cyclone, separation efficiency was controlled by the ($density_{particle}$ - $density_{water}$)/$viscosity_{water}$ ratio. Because this ratio is sensitive to temperature, especially in the neighborhood of the supercritical point, separation efficiencies sharply increased with temperature. Contrary to traditional air cyclone theory, removal efficiency was inversely correlated to flow rate. This result was caused by particle deposition and particle flocculation in the

* To whom correspondence should be addressed.

heater. Low flow rates increased heater detention times and, thus, opportunities for flocculation and particle deposition. Therefore, the performance of a hydrocyclone used in conjunction with supercritical oxidation depends on phenomena occurring in the heater and the hydrocyclone.

INTRODUCTION

Supercritical water oxidation (SCWO), a process that involves oxidation of organics above the critical temperature (374.2°C) and pressure (22.1 MPa) of water, is a relatively new treatment technology for the destruction of organic compounds in wastewaters and sludges. Above the critical point, water exists as a supercritical fluid, exhibiting several unique properties, such as rapid reductions in its density and viscosity (6). Inorganic particles and salts may be produced when wastes are treated hydrothermally (11); such particles consist of hard, dense metal oxides than can have destructive effects to downstream equipment. They can be abrasive to pressure regulators, thermocouples, and pressure transducers, and can cause erosion of tubing walls and scaling of heat exchangers, thus making their removal from the SCWO effluent essential.

We studied the performance of a hydrocyclone particle-separation system for conditions relevant to a supercritical water oxidation process. The hydrocyclone is a high efficiency separation device that can work effectively in the high temperatures and pressures required by the supercritical water environment. It is economical and, having no moving parts, requires little maintenance. In its simplest form, a cyclone consists of a cylindrical shell fitted with a tangential inlet (feed port), an axial exit pipe (overflow port) for the cleaned effluent, and a conical base with solids discharge through the underflow port.

Cyclone performance in high temperature and pressure environments has been studied before (15), and the separation of particles from supercritical water oxidation effluents was studied by Dell'Orco (2). Our objective was to study the performance of a hydrocyclone particle separation system when used in conjunction with a heater in a supercritical water oxidation process. We assessed the effects of the heater on the particle removal capability of the hydrocyclone for a range of temperatures and flow rates. We also obtained particle size distributions to study the effect of particle size on removal for different experimental conditions.

BACKGROUND

A cyclone is a settling chamber in which gravitational acceleration is replaced by centrifugal acceleration (13). Inertia causes the particles to move toward the outside cylinder wall, where they are carried down with the fluid. According to Stairmand (16), the centrifugal and inward viscous forces just balance for a particle of a given density when the particle has its critical size;

then, the particle moves neither outward to the walls nor inward to the cyclone axis. All particles larger than this critical size (also referred to as the "cut" of the cyclone under the given conditions) should be collected, and all smaller particles should escape. In practice, however, a considerable number of particles smaller than the "cut" are separated with the coarser particles, possibly due to agglomeration and sweeping of smaller particles by larger ones. Also, some particles coarser than the "cut" are carried into the inner vortex by eddies or by bouncing off the walls, and they escape with the smaller particles through the overflow port.

An efficiency expression that does not involve the underflow stream and is based on the feed and overflow stream concentrations (c_0 and c, respectively) is termed collection or removal efficiency, η, and is defined as

$$\eta = (c_0 - c)/c_0 \tag{1}$$

The relationship between collection efficiency and particle size for a given particle type and a given collector is called the "grade efficiency" or "fractional efficiency" (14), which normally is expressed in graphical form by plotting removal efficiency against log d_p, where d_p is the particle diameter. In practice, the grade efficiency curve usually has an "S" shape, or a gradual rise at the cyclone "cut" that asymptotically approaches a maximum value (expected to be 1).

The models that have been developed to predict efficiency for hydrocyclones use operating parameters of the system to predict performance, and many of them account for the influence of particle diameter and density, as well as fluid velocity and viscosity. Leith and Licht (14) developed a model that provides insight into what drives the particle separation in a cyclone. The expression for grade efficiency for a given particle size (i.e., η_g) is

$$\eta_g = 1 - \exp[-2(C\Psi)^{1/(2n+2)}] \tag{2}$$

The term C is a dimensionless geometry parameter (not presented herein) that is a constant for any cyclone design, with each cyclone having a unique value of C. The particle and fluid properties are grouped in Ψ, a modified inertia parameter:

$$\Psi = \frac{(\rho_p - \rho_f) d_p^2 \upsilon_i (n + 1)}{18 \mu D} \tag{3}$$

where ρ_p and ρ_f are the densities of particle and fluid, respectively, υ_i is the inlet fluid velocity, μ is the fluid viscosity, D is the cyclone body diameter, and n is the vortex exponent, which is defined below. According to Eqs. (2) and (3), separation efficiency for a given flow rate and a given particle size is expected to increase as the ratio $(\rho_p - \rho_f)/\mu$ increases. Other models in the literature (2, 3) also agree on the significance of this ratio on cyclone efficiency.

MARCEL DEKKER, INC.
270 Madison Avenue, New York, New York 10016

Since the density and viscosity of water decrease dramatically as water enters the supercritical phase, the numerator of the ratio increases and the denominator decreases, making the ratio and, consequently, the separation efficiency increase sharply with increasing temperature. Figure 1 shows that ratio as a function of temperature near the critical point of water at 27.6 MPa, which is the pressure for all experiments of this research. Efficiency is also expected to increase as the flow rate increases because of the term ν_i in the numerator of Eq. (3). The vortex exponent n, defined as

$$n = 1 - [(1 - 0.67D^{0.14})(T/283)^{0.3}] \quad (4)$$

also is temperature-dependent. However, the temperature effects of n on η_g are minor when compared to the effect of the ratio $(\rho_p - \rho_f)/\mu$.

Previous researchers who used our pilot plant (2, 11) suggested that a significant percentage of the feed particles were trapped by deposition in the heater. The phenomenon of particle deposition, or fouling, on heater surfaces is described in the literature (4, 5), and we decided to investigate it theoretically and experimentally. In theory, the spatial distribution of free charges surrounding a charged particle is usually idealized as an electric double layer, with one layer viewed as a fixed charge attached to the particle while the other is diffusely distributed in the liquid in contact (Gouy–Chapman diffuse model) (18). Gasparini et al. (8–10) invoked electrical double-layer effects to explain several observations of metal oxides (like alumina) depositing on negatively charged steel surfaces (like the SCWO unit heater). The negatively charged oxides appear positive due to the fixed layer of positive charge attached on the particle and are attracted by the negatively charged steel surfaces.

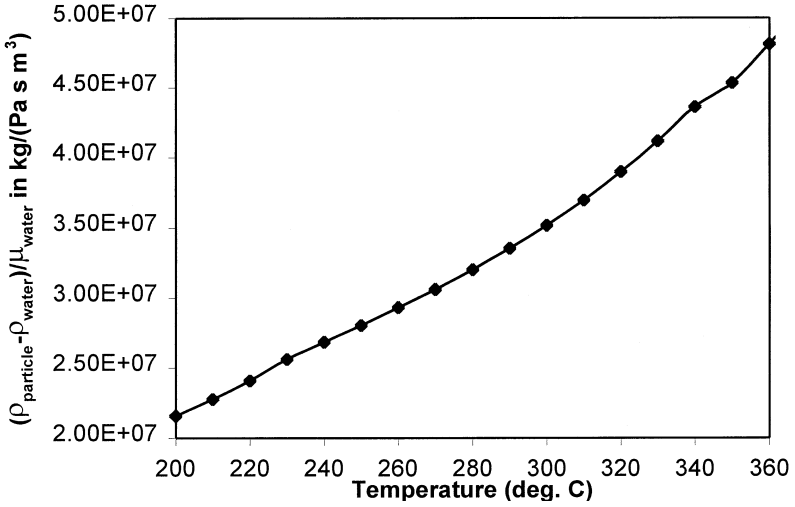

FIG. 1 Ratio of $(\rho_p - \rho_f)/\mu$ for water as a function of temperature near the critical point at 27.6 MPa.

MARCEL DEKKER, INC.
270 Madison Avenue, New York, New York 10016

EXPERIMENTAL METHODS

Experimental Apparatus

We performed pilot-scale experiments to evaluate the particle-separation capabilities of a hydrocyclone coupled to a heating system. A 150-kg/h pilot plant with a specially designed heater/hydrocyclone apparatus was used. The main components of the particle-separation system were the feed-distribution system, the heating system, and the hydrocyclone.

Part of the feed-distribution system was a 965-L tank used as the feed reservoir. Distilled deionized water was fed directly into the tank. A mechanical mixer mounted on the lid of the tank, along with a grinder pump, ensured adequate mixing of the feed solution. A centrifugal pump provided the necessary inlet net positive suction head for the diaphragm feed pump, which controlled the flow rate in the system. A series of valves and flowmeters ensured the smooth operation of the feed distribution system.

The heating system included two 6.6-m long heat exchangers that were used to preheat the feed stream by using the heat recovered from the effluent stream. The feed solution was heated to the desired temperature, while the feed temperature was controlled at the heater outlet using a thermocouple that was connected to a Fisher Porter Process Control System. To ensure minimal heat loss, all the heating equipment and the tubing were heavily insulated with thick layers of Kaowool ceramic fiber insulation.

The hydrocyclone comprised a 25.4-mm diameter cyclone and an underflow receiver. The hydrocyclone, designed in accordance with the work of Haas et al. (12), is shown in Fig. 2. The underflow receiver was a 2.2-m long vessel (1 gallon capacity) connected to the underflow port of the cyclone. To achieve temperature uniformity of the underflow port so that particle reentrainment in the cyclone did not occur, two ceramic tubular heaters were used. Figure 3 shows how the cyclone apparatus was integrated with the heating system. The dashed line shown in Fig. 3 was used for Exp. T13, when the hydrocyclone was bypassed, and heater effluent was sampled at the overflow sampling point.

Experimental Procedures

Initially, water was fed to the pilot unit until the desired temperature and pressure conditions were established. This process took anywhere from 1 to approximately 5 hours, depending on the desired temperature. Once the desired conditions were established, the feed stream was changed to the particles suspension. At this point the feed pump was adjusted to the desired flow rate, and, once that flow rate was established, approximately 20 minutes were allowed for the system to achieve temperature equilibrium.

During one day's run, temperature and pressure were kept constant, while the flow rate was varied three times. Three replicate samples were taken at

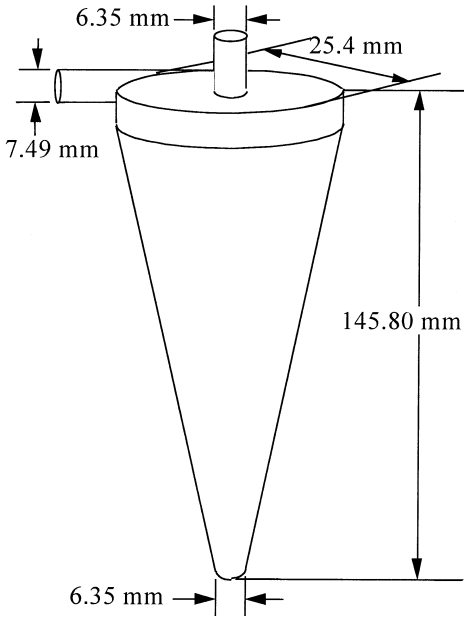

FIG. 2 Hydrocyclone internal dimensions.

each set of conditions, and these samples were taken at approximately 10-minute intervals. After all samples for one flow rate were taken, the pump was adjusted to the new flow rate, and the replicate samples were taken for the new flow rate. After each day's experiment the system was rinsed with water until the effluent was clear. When the system had cooled down to approximately room temperature, the underflow pot was emptied and rinsed until the appearance of the effluent was clear. The underflow pot's contents and rinsewater were collected, and samples were taken.

Experimental Conditions

The particulate matter that was used to study the separation capabilities of the hydrocyclone was monocrystalline α-alumina powder (Electronic Grade Precision Alumina, Grain Code 7921, Norton Company) with a mean mass diameter of 3.60 μm, according to the manufacturer. The effects of several independent variables on particle removal were investigated. The variables under direct control were temperature and flow rate. Four temperature-variation experiments were performed with temperatures ranging between 25 and 340°C and with the feed concentration constant at 500 mg/L (25°C, Exp. T11; 150°C, Exp. T6; 260°C, Exp. T7; and 340°C, Exp. T9). For each temperature, three flow rates (0.0126, 0.0202, and 0.0296 L/s) were investigated. For all experiments the pressure was held constant at 27.6 MPa. Three replicates were obtained at each set of conditions.

To investigate experimentally the particle removal due to heater fouling rather than due to the hydrocyclone, an additional experiment was run at 260°C (feed concentration = 500 mg/L) for the three flow rates with the hydrocyclone excluded from the system (Exp. T13).

Experimental Analysis

Two types of analyses were performed: particle-size distributions and total suspended solids. Suspended solids were measured according to Method

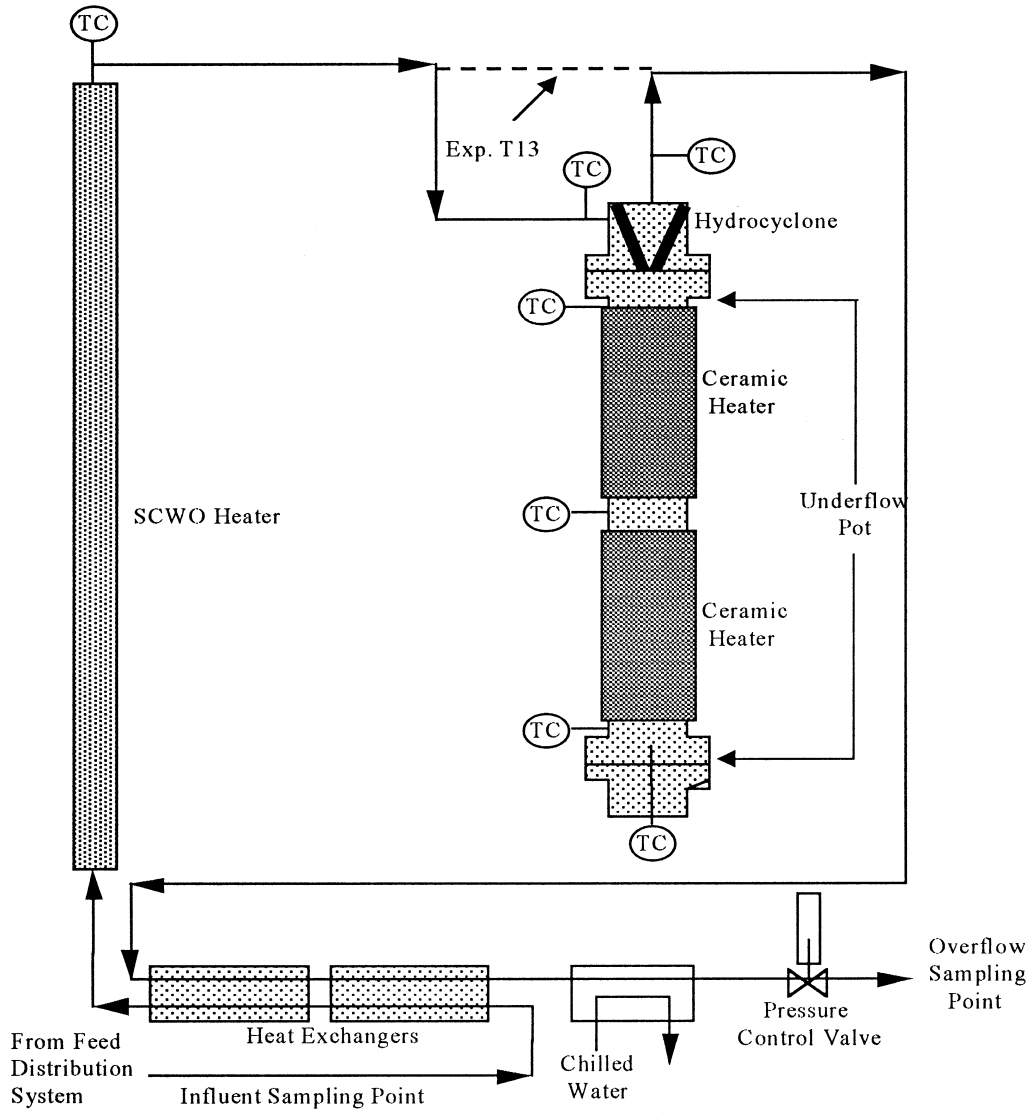

TC: thermocouple

FIG. 3 Schematic of the heating system connected to the hydrocyclone apparatus.

MARCEL DEKKER, INC.
270 Madison Avenue, New York, New York 10016

2540D of *Standard Methods for the Examination of Water and Wastewater* (17). Total suspended solids were analyzed for all samples. The three replicate samples obtained for each condition were averaged, and the standard deviation was computed. For each condition the one replicate that was closest to the average was chosen for particle-size analysis.

Particle-size distributions were measured with an electronic particle counter (Coulter Multisizer, Coulter Electronics, Hialeah, FL) that uses the principle of electrical resistivity and responds to particle volume. Each sample was analyzed with two different aperture sizes (30 and 100 μm). A standard setting on the particle counter was used throughout this research, so that each channel represented a logarithmic increment of particle diameter of 0.012 (i.e., $\Delta \log d_p = 0.012$ for all channels). Each aperture measures particle sizes that range from approximately 3 to 20% of the aperture diameter, which means that a significant amount of overlap exists in the particle sizes measured by the two apertures. This overlap was used to verify data quality; similar number concentrations should be obtained for a given particle size regardless of the aperture used for analysis. In the data reported, the 30-μm aperture was used for particles in the 1.0 to 2.8 μm range ($0.0 < \log d_p < 0.45$), and the 100 μm aperture was used for the 2.8 to 12 μm range ($0.45 < \log d_p < 1.1$). Counts above a log d_p of 1.2 were considered suspect due to low particle counts. Good agreement between both apertures was achieved for most samples run by the Coulter Counter; such agreement is an indicator of good quality measurements.

RESULTS AND DISCUSSION

Total Suspended Solids Data

Mass balances, based on total suspended solids data, were completed for all experimental runs. These mass balances were taken around the heater/hydrocyclone system. The concentrations of the feed, overflow, and underflow (C_f, $C_{o,i}$, and C_u, respectively) were obtained from the suspended-solids analyses. Three overflow concentrations corresponded to each experimental run—one for every flow rate. The volumes V_f, $V_{o,i}$, and V_u were obtained from the flowmeter recording of the cumulative mass of alumina suspension fed to the system. Then, the percentage of solids recovered was computed by

$$\% \text{ Solids recovered} = \frac{\text{total mass of solids out}}{\text{total mass of solids in}} = \frac{\sum_{i=1}^{3} (C_{o,i}V_{o,i}) + C_u V_u}{C_f V_f} \quad (5)$$

For Run T13, $C_u V_u = 0$, since the hydrocyclone was excluded. The percentages of solids recovered for all the experiments, shown in Table 1, are close to

TABLE 1
Mass Balances for Heater–Hydrocyclone Experiments (all experiments at an initial feed concentration of 500 mg/L)

Experiment	Temperature (°C)	Solids recovered (%)
T11	25	98.41
T6	150	79.67
T7	260	80.91
T10	260	80.07
T13[a]	260	79.30
T9	340	81.07

[a] Hydrocyclone not included in the apparatus.

80%, except for the room temperature Exp. T11, for which solids recovery is almost 100%. These results confirmed what other researchers (2, 11) had previously reported, i.e., a significant mass of particles (approximately 20% of the feed on a weight basis) deposits on the heater surface and, therefore, never reaches the hydrocyclone influent or the underflow pot.

System removal efficiencies (η, Eq. 1) were calculated for all experimental conditions, and the effects of temperature and flow rate are shown in Fig. 4. At each temperature the system's removal efficiency declined with increasing flow rate, but increased dramatically with increasing temperature. Temperature effects agree with hydrocyclone theory, but flow rate effects are counter.

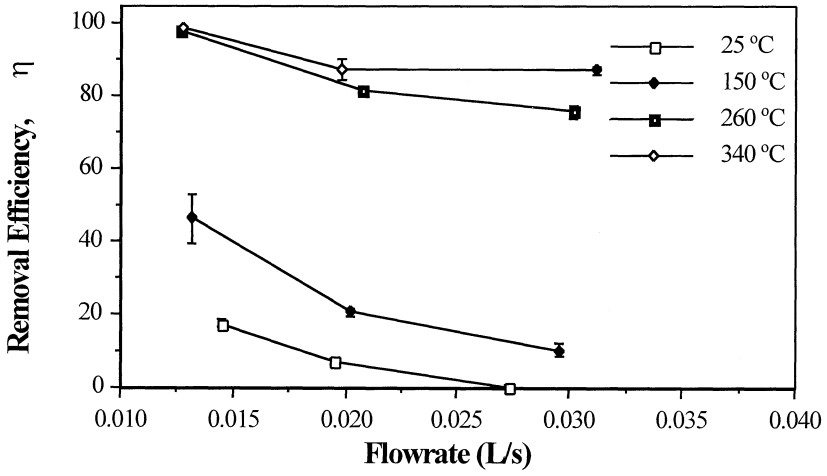

FIG. 4 Removal efficiency for the system as a function of flow rate and temperature (all experiments at an initial feed concentration of 500 mg/L).

MARCEL DEKKER, INC.
270 Madison Avenue, New York, New York 10016

Particle-Size Data

Heater Effects

To investigate the effect of flow rate on particle removal in the heater alone, we analyzed particle-size distributions on the overflow samples of Exp. T13 (hydrocyclone excluded) at three different flow rates. The results, shown in Fig. 5, demonstrate that small particles were lost in the heater. The ordinate values represent the number concentration of particles within an incremental size range, normalized by that incremental size range. Each number increment is plotted versus the log of particle diameter (d_p in μm) using the value of the midpoint of the incremental log size range. The removal or gain of a particle of a given size is shown by a vertical difference from the feed. Differences in slopes among different samples indicate the selective removal or creation of particles over different size ranges.

The loss of small particles occurred in all runs, but was greatest at the slowest flow rate, since the distribution that corresponds to the slowest flow rate is positioned lower than all other distributions for $\log d_p \leq 0.8$. The particle-size distributions also document that flocculation of the alumina particles was taking place in the heater. Compared to the feed, the overflow had a higher concentration of the largest particles, $\log d_p > 0.8$.

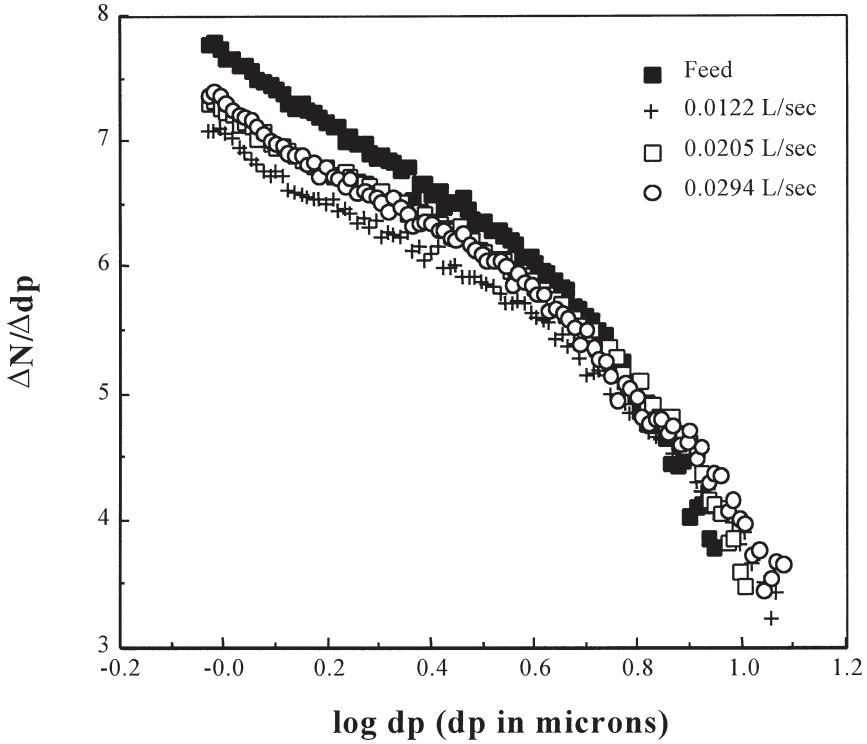

FIG. 5 Particle size distributions of Exp. T13 (260°C, by passing the hydrocyclone).

MARCEL DEKKER, INC.
270 Madison Avenue, New York, New York 10016

The loss of particle volume in the small sizes was not completely balanced by the gain in the large sizes, as one would expect from flocculation alone. To quantify this, we summed the vertical differences between the feed distribution and two of the flow-rate distributions (0.0294 and 0.0122 L/s) over the whole size range. The feed distribution was higher than the 0.0122 L/s distribution by 0.406 units for $0 < \log d_p < 0.84$ μm, while the latter distribution is higher than the former by only 0.043 units for $0.84 < \log d_p < 1.068$ μm. Similarly, the feed distribution is higher than the 0.0294 L/s distribution by 0.221 units for $0 < \log d_p < 0.77$ μm, while the latter distribution is higher than the former by only 0.090 units for $0.77 < \log d_p < 1.08$ μm. These results agree with the TSS mass balance (Table 1) and add further evidence of deposition on the walls.

According to Garrett-Price et al. (7), the loss of particles due to heater fouling increases as the flow rate decreases, since opportunities for deposition of particles increase with increasing detention time. Additionally, the laminar boundary layer adjacent to the walls should be thicker at the lower flow rate, reducing the likelihood of scouring the walls, leading to particle reentrainment.

The removal of fine particles in the heater dramatically altered the particle-size distribution of the hydrocyclone inflow stream, therefore altering the observed removals of the hydrocyclone. According to cyclone theory, removal-efficiency curves have an "S" shape, showing that particles smaller than the "cut" of the cyclone are not collected, while particles larger than the "cut" are well collected. With the heater preferentially removing the smaller particles that would otherwise not be collected by the cyclone, removal efficiencies across the hydrocyclone appear enhanced, especially for lower flow rates, when heater fouling is magnified. To differentiate the removal efficiencies in the cyclone from the particle removal in the heater, we combined the results from Exp. T7 (whole system) and Exp. T13 (heater alone). These experiments were performed at the same temperature and pressure and with the same feed concentration. Figure 6 presents the removal efficiency according to particle size. Due to flocculation and preferential removal of fine particles in the heater, the heater removal curve is the highest for small $\log d_p$ values. The hydrocyclone-only removal curve has reduced removal efficiencies for the small particles, although the curve does not take the classic "S" shape. The removal curve for the whole system is relatively constant, particularly for the small particles. The total-system removal declines for $\log d_p > 0.8$, even though the removal efficiency by the hydrocyclone is at its highest. The creation of large particles by flocculation in the heater means that the total-system removal is less than the hydrocyclone removal for $\log d_p > 0.9$.

Effects of Flow Rate

The particle volume distributions of the feed, the overflow samples collected at each flow rate, and the underflow samples for Exp. T6 (150°C) are

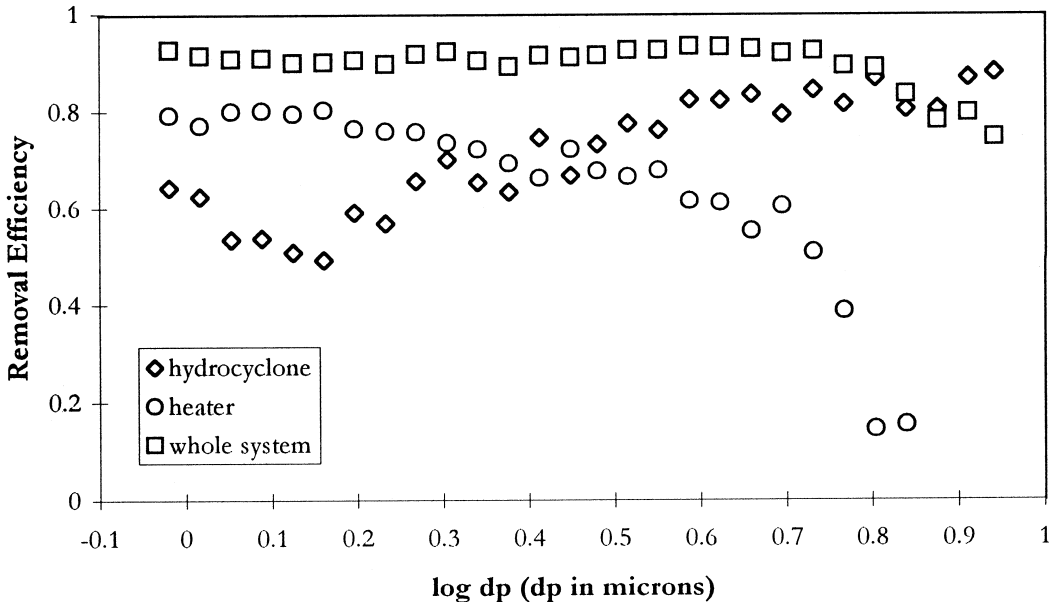

FIG. 6 Grade-efficiency curves at 260°C and 0.0127 L/s for the whole system, the hydrocyclone, and the heater alone.

shown in Fig. 7. Here, the ordinate values represent volume concentrations in a log size range, normalized by that log range, and particle removal is manifested by area differences. Experiment T6 shows trends typical of the other experiments.

For the feed sample, Part (A) of Fig. 7, almost all of the particle volume was contained in particles with log d_p between 0.0 and 1.0 (d_p between 1.0 and 10.0 μm). The same was true for the feed samples of all experiments, since the same feed material was used in all experiments. Also, the peak in the volume distribution between $0.6 \leq \log d_p \leq 0.8$ (4.0 μm $\leq d_p \leq$ 6.3 μm) was common to all feed samples.

Volume distributions of the three overflow samples (one for each flow rate tested) of Exp. T6 are shown in Part (B) of Fig. 7. The effects of flow rate on removal efficiency can be seen from these distributions. Higher flow rates resulted in distributions that peak at higher ordinate values and have higher concentrations throughout the entire size range. An increasing flow rate resulted in lower removal efficiencies overall and a significant increase in particles in the range $0.4 < \log d_p < 0.9$. The same effect of flow rate on removal efficiency was observed in all experiments; that is, for all temperatures the highest particle removals were observed at the lowest flow rate and vice versa.

The volume distribution of the underflow sample is shown in Part (C) of Fig. 7. The ordinate values of this distribution are much higher than those of the feed because the volume concentration of the underflow was higher than

that of the feed. The particle-size distribution of the underflow is shifted to larger sizes in comparison to the distribution of the feed (Part A). Such a shift is an indicator of the size effect on capture: larger particles were removed preferentially by the hydrocyclone.

The effects of flow rate on removal efficiency also can be seen in grade-efficiency curves (i.e., the removal efficiency as a function of particle size).

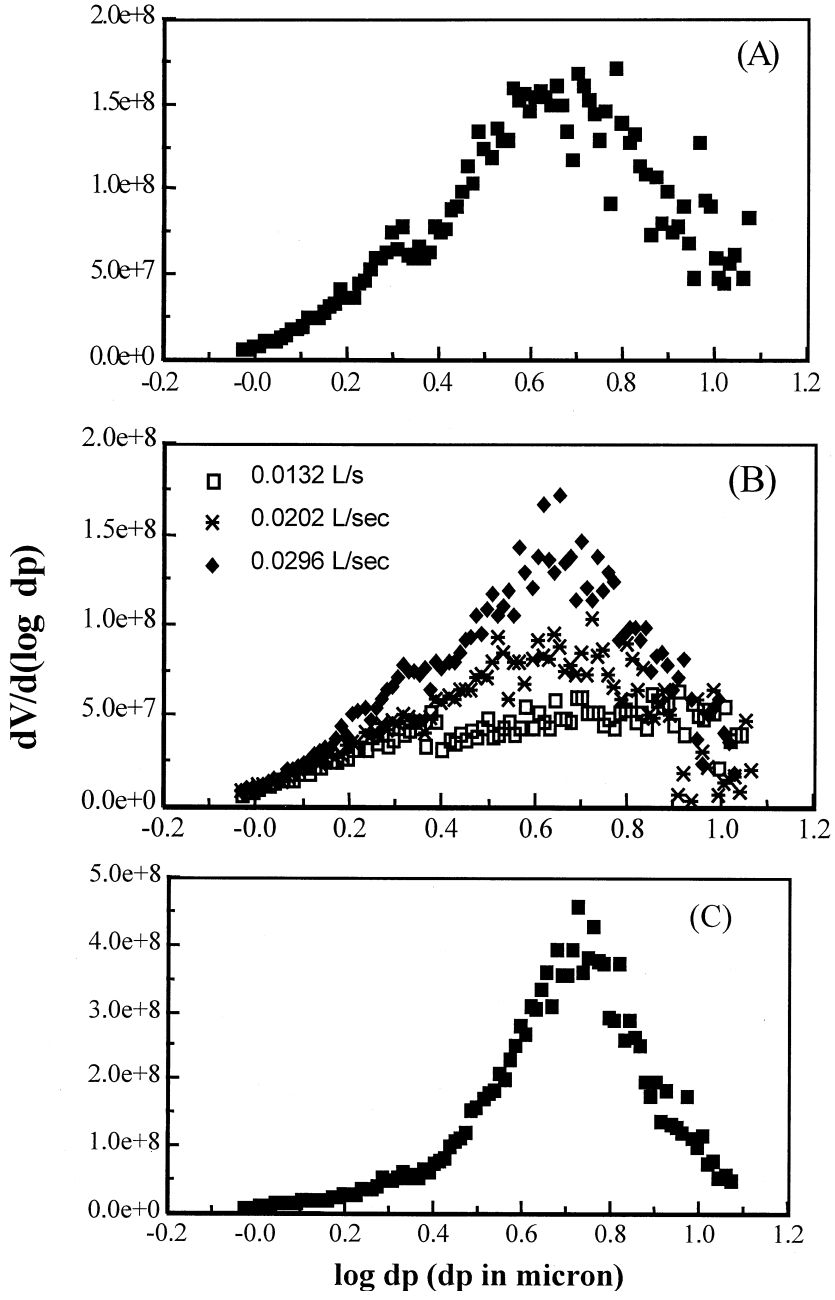

FIG. 7 Volume distributions of Exp. T6 (150°C): (A) feed, (B) overflow, (C) underflow.

MARCEL DEKKER, INC.
270 Madison Avenue, New York, New York 10016

Figure 8 shows the grade-efficiency curves for Exp. T6 (150°C). Increasing flow rates (i.e., Parts A to B to C) move the curve downward, or to lower efficiencies, for particle sizes up to about log $d_p \approx 0.9$.

According to traditional theories of cyclone performance, such as Eq. (2), the separation efficiency should increase as flow rate increases. Thus, our results contradict traditional theory concerning the effect of flow rate. The poor predictive power of the traditional models may occur in part because the models were developed primarily for air cyclones, not for high-temperature and pressure hydrocyclones. Even more important is that the heater, by preferentially removing smaller particles and by inducing flocculation, especially for low flow rates, dramatically alters the particle-size distributions of the stream influent to the hydrocyclone. The effects of the heater on the particle-size distribution should not be viewed as merely an artifact, since the heater is an integral part to any system in which the hydrocyclone is used in conjunction with supercritical extraction. In other words, the effects of flow rate on removal by the hydrocyclone in high-temperature environments, when a heater has to be used, should not be expected to agree with theoretical models, since removal of fine particles and flocculation in the heater occur, particularly at low flow rates. Since the heater preferentially removes small particles, which the cyclone is least able to remove, the effects of flow rate contradict hydrocyclone theory when the hydrocyclone is coupled to a heater.

In Part (A) of Fig. 8, we observe that, although the curve has the expected "S" shape, an unexpected drop in the efficiency is shown for log $d_p > 0.6$ ($d_p > 4.0$ μm). Such drops in the efficiency were also observed by Williamson et al. (19), who attributed them to small errors in size analysis that become magnified in calculations relating to low particle numbers in particular size ranges. That explanation might be acting in those experiments as well, but an alternative explanation is more important. The formation of new larger particles due to flocculation in the heater resulted in an increased loading of larger particles to the hydrocyclone, therefore lowering the removal efficiency of the system for that size range. Flocculation was the greatest at the lowest flow rate, which is consistent with the fact that such a drop in the efficiency curve is only observed at the lowest flow rate (Part A of Fig. 8).

Effects of Temperature

For all flow rates, increasing temperatures resulted in higher separation efficiencies. Figure 9 illustrates this trend by comparing the grade-efficiency curves for 25, 150, and 340°C. The curves clearly move upward to higher efficiencies as temperature increases. This observation agrees well with the suspended solids data (Fig. 4) that showed a strong dependence on temperature, with removals at low temperatures equal to almost zero, while removals at high temperatures reach almost 100%.

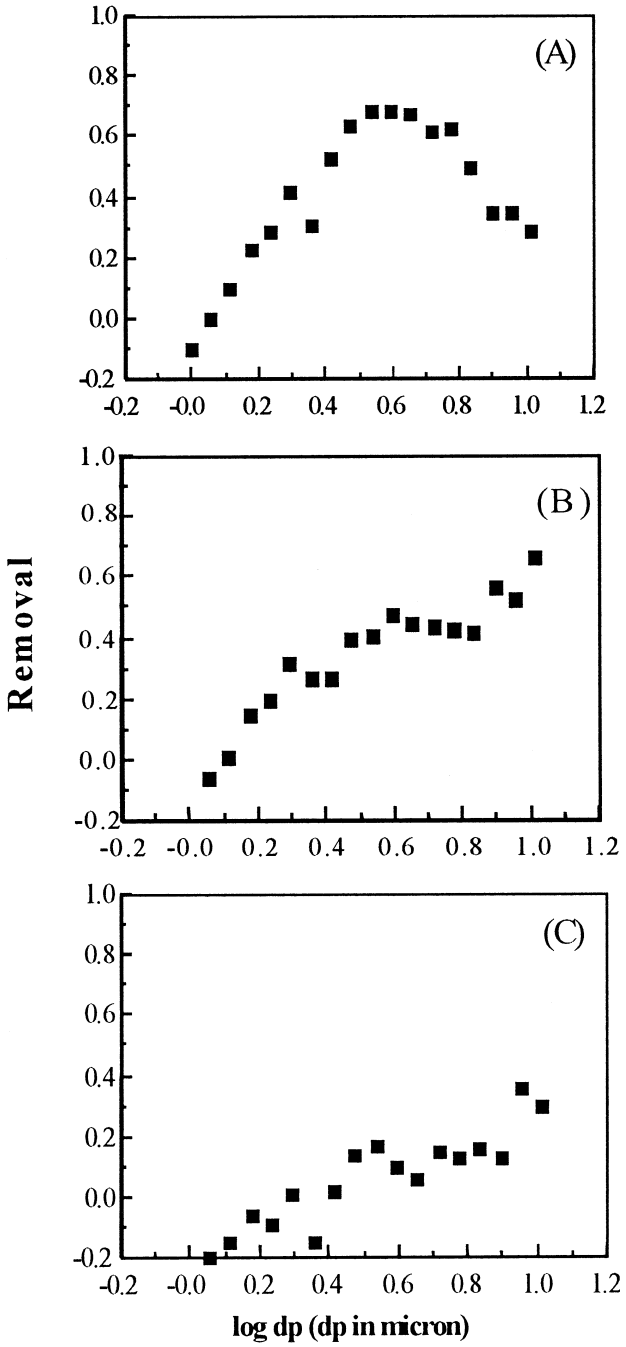

FIG. 8 Grade-efficiency curves for the system: Effect of flow rate. All results shown taken from Exp. T6 (150°C). (A): 0.0132 L/s, (B): 0.0202 L/s, (C): 0.0296 L/s.

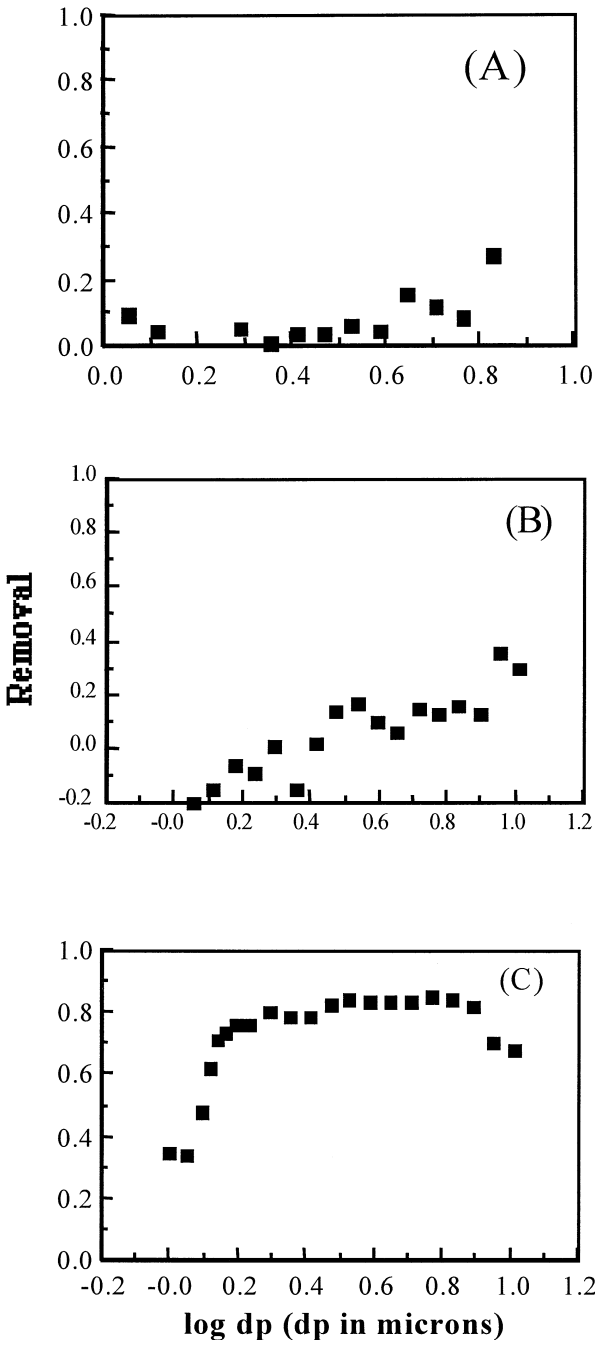

FIG. 9 Grade-efficiency curves for the system: Effect of temperature. All experiments are at a flow rate of 0.0296 L/s. (A): Exp. T11 (25°C), (B): Exp. T6 (150°C), (C): Exp. T9 (340°C).

As shown in the Background section, separation efficiency should increase with increasing temperature, since the ratio $(\rho_p - \rho_f)/\mu$ increases with temperature. Thus, the observed trend of hydrocyclone removal is in agreement with the theory for temperature.

CONCLUSIONS

A 25.4-mm hydrocyclone was effective in removing α-alumina particles from water at elevated temperatures and pressures. The removal efficiency of the hydrocyclone was very sensitive to temperature. Removal efficiencies based on total suspended solids data ranged from less than 20% at 25°C to 90–99% at 340°C. The temperature sensitivity is due mainly to the dependence of the hydrocyclone separation efficiency on the ratio $(\rho_p - \rho_f)/\mu$, which dramatically increases with temperature, especially in the neighborhood of the water's supercritical point.

Increased flow rate resulted in lower removal efficiencies, contrary to traditional air cyclone theory. The cause of this observed trend was particle flocculation and trapping in the heater preceding the hydrocyclone. Lower flow rates resulted in higher detention times in the heater, increasing the opportunities for particle flocculation and attachment on the heater surface. Suspended solids measurements and particle-size distributions revealed that flocculation and particle trapping were indeed significant. When the hydrocyclone was by-passed for the purpose of studying the heater effects on particle removal, flocculation was clearly indicated by the loss of small particles and the increase in large particles. In addition, about 20% removal was observed, mainly from the smallest particle sizes. In summary, the performance of the hydrocyclone system used as posttreatment for supercritical oxidation depends on particle removal and flocculation that occur in the heater, as well as to separation in the hydrocyclone.

REFERENCES

1. D. Bradley, *The Hydrocyclone*, Pergamon Press, New York, NY, 1965.
2. P. C. Dell'Orco, "The Separation of Particles from Supercritical Water Oxidation Effluents," M.S. Thesis, The University of Texas at Austin, Austin, TX, 1990.
3. L. Enliang and W. Yingmin, *AIChE J.*, *35*, 666 (1989).
4. N. Epstein, *Heat Transfer 1978*, Vol. 6, Hemisphere, New York, NY, 1978, p. 235.
5. N. Epstein, in *Fouling of Heat Transfer Equipment* (E. F. C. Somerscales and J. G. Knudsen, Eds.), Hemisphere, Washington, DC, 1981, p. 31.
6. E. W. Frank, in *High Temperature, High Pressure Electrochemistry in Aqueous Solutions* (NACE-4), 1976, p. 109.
7. B. A. Garrett-Price, S. A. Smith, R. L. Watts, J. G. Knudsen, W. J. Marner, and J. W. Suitor, *Fouling of Heat Exchangers*: *Characteristics*, *Costs*, *Prevention*, *Control and Removal*, Noyes Publications, Park Ridge, NJ, 1985.

MARCEL DEKKER, INC.
270 Madison Avenue, New York, New York 10016

8. R. Gasparini, C. Della Rocca, and E. Ioannilli, *Combustion*, *41*(5), 12 (1969).
9. R. Gasparini, C. Della Rocca, and E. Ioannilli, *Corros. Sci*., *10*, 157 (1970).
10. R. Gasparini and E. Ioannilli, *Proc. Am. Power Conf.*, *33*, 776 (1971).
11. M. G. E. Goemans, "The Separation of Inorganic Salts and Metal Oxides from Supercritical Water by Cross-Flow Microfiltration," Master's Thesis, The University of Texas at Austin, Austin, TX, 1993.
12. P. A. Haas, E. O. Nurmi, M. E. Whatley, and J. R. Engel, *Hydraulic Cyclones for Application to Homogeneous Reactor Chemical Processing* (ORNL-2301), 1957.
13. W. R. Killilea, G. T. Hong, K. C. Swallow, and T. B. Thomason, *Supercritical Water Oxidation*: *Microgravity Solids Separation* (SAE Technical Paper Series, No. 881038), 1988.
14. D. Leith and W. Licht, *AIChE Symp. Ser*., 126, *68*, 196 (1972).
15. R. Parker, R. Jain, S. Calvert, D. Drehmel, and J. Abbott, *Environ. Sci. Technol*., *15*(4), 451 (1981).
16. C. J. Stairmand, *Trans. Inst. Chem. Eng. 29*, 356 (1951).
17. *Standard Methods for the Examination of Water and Wastewater*, 19th ed. (A. D. Eaton, L. S. Clesceri, and A. E. Greenberg, Eds.), American Public Health Association, Washington, DC, 1995.
18. W. Stumm, *Chemistry of the Solid–Water Interface*, Wiley, New York, NY, 1992.
19. R. D. Williamson, T. R. Bott, H. S. Kumar, and I. H. Newson, *Sep. Sci. Technol*., *18*(12& 13), 1395 (1983).

Received by editor November 17, 1998
Revision received February 1999

Request Permission or Order Reprints Instantly!